

Evaluated Photonuclear Data Library in KAERI

Young-Ouk Lee, Yinlu Han¹, Jeong-Yeon Lee and Jonghwa Chang
*Korea Atomic Energy Research Institute
P.O. Box 105 Yusong, Taejon 305-600, Korea*

abstract

Based on available experimental data of photonuclear reaction and theoretical models, an evaluated photonuclear data library is provided for a variety of applications up to 140 MeV. The photoabsorption cross section is evaluated with the giant dipole resonance model and quasideuteron model, and production cross section and emission spectra for neutron, proton, deuteron, triton, alpha particles, gamma rays, and all residual nuclides produced ($A \geq 5$) in the reaction chains were calculated with the Hauser-Feshbach statistical, preequilibrium and multiple-preequilibrium theories by GNASH. The calculated results of photonuclear reaction data were analysed and compared with existing experimental data. Total 142 isotopes of 39 elements were included in the evaluated photonuclear data library, and the cross sections are stored in ENDF/B-VI format.

I. Introduction

There is a recent interest in developing evaluated photonuclear data libraries for photon energies up to 140 MeV, since photonuclear reaction cross section data are of importance for a variety of applications such as

- radiation protection and dosimetry of photoneutron produced by electron or photon accelerators in medical applications,
- calculations of absorbed dose in a human body during radiotherapy,
- physics and technology of fission reactors and fusion reactors,
- activation analysis, safeguards and inspection technologies,
- nuclear waste transmutation, and
- astrophysics.

However, in general, there is a substantial lack of evaluated photonuclear data. In this situation, these activities have relied heavily on nuclear model calculations which are benchmarked to available measurements.

KAERI is building a photonuclear data library with international collaboration by participating in the IAEA's Coordinated Research Project (CRP) under the title "Compilation and evaluation of photonuclear data for applications" since 1997. Currently 142 isotopes of 39 elements were included in the KAERI photonuclear data library [1–8]. The recommended photonuclear data were obtained based on experimental data and theoretical calculated data up to an incident photon energy of 140 MeV which is the threshold energy for pion production. The decaying processes including neutron, proton, deuteron, triton and alpha particles were theoretically calculated up to 140 MeV by the GNASH code[9].

¹Permanent Address: China Institute of Atomic Energy

The status of the evaluated photonuclear library is presented in Sec. II and library data format is given in Sec. III. The theoretical models and evaluation techniques applied in this work are described in Sec. IV. Evaluation procedures for some selected isotopes are presented in Sec. V. Finally, we give a brief summary in Sec. VI.

II. The Status of Evaluated Photonuclear Data Files

The photonuclear data are important for a variety of applications. According to the most important data requested, isotopes of 39 elements were included in the evaluated photonuclear data library as follows:

Structural, Shielding and Bremsstrahlung Target Materials

$_{13}\text{Al}^{27}$, $_{24}\text{Cr}^{50,52,53,54}$, $_{25}\text{Mn}^{55}$, $_{27}\text{Fe}^{54,56,57,58}$, $_{27}\text{Co}^{59}$, $_{28}\text{Ni}^{58,60,61,62,64}$, $_{29}\text{Cu}^{63,65}$,
 $_{30}\text{Zn}^{64,66,67,68,70}$, $_{40}\text{Zr}^{90,91,92,94,96}$, $_{42}\text{Mo}^{92,94,95,96,97,98,100}$, $_{50}\text{Sn}^{112,114,115,116,117,118,119,120,122,124}$,
 $_{52}\text{Te}^{120,122,123,124,125,126,128,130}$, $_{59}\text{Pr}^{141}$, $_{67}\text{Ho}^{165}$, $_{79}\text{Au}^{197}$, $_{83}\text{Bi}^{209}$.

Biological Materials

$_{6}\text{C}^{12,13}$, $_{7}\text{N}^{14,15}$, $_{8}\text{O}^{16,17,18}$, $_{11}\text{Na}^{23}$, $_{16}\text{S}^{32,33,34,36}$, $_{17}\text{Cl}^{35,37}$, $_{20}\text{Ca}^{40,42,43,44,46,48}$.

Nuclear Waster Transmutation

$_{38}\text{Sr}^{84,86,87,88,90}$, $_{40}\text{Zr}^{93}$, $_{41}\text{Nb}^{93,94}$, $_{46}\text{Pd}^{102,104,105,106,107,108}$, $_{47}\text{Ag}^{107,108,109}$, $_{53}\text{I}^{127,129}$,
 $_{55}\text{Cs}^{133,135,137}$, $_{62}\text{Sm}^{144,147,148,149,150,151,152,154}$, $_{65}\text{Tb}^{158,159}$.

Actvation Analysis

$_{14}\text{Si}^{28,29,30}$, $_{18}\text{Ar}^{36,38,40}$, $_{19}\text{K}^{39,40,41}$, $_{22}\text{Ti}^{46,47,48,49,50}$, $_{32}\text{Ge}^{70,72,73,74,76}$, $_{46}\text{Pd}^{110}$,
 $_{48}\text{Cd}^{106,108,110,111,112,113,114,116}$, $_{51}\text{Sb}^{121,123}$.

Astrophysics

Nuclei such as $_{14}\text{Si}^{27}$, for use as a cosmological chronometer.

The evaluation provides a complete representation of the nuclear data needed for a variety of applications over the incident photon energy range from 7 to 140 MeV which is the threshold energy for pion production.

III. The Photonuclear Data Format

The ENDF/B-VI format is the internationally recognized standard format to store evaluated nuclear reaction data for applications, and uses a hierarchical organization of information. The format adopted for photonuclear data is summarized in Table 1.

IV. Theoretical Models and Evaluation Techniques

The photoabsorption cross sections are important in photonuclear reaction cross sections. The Giant-Dipole Resonance (GDR) and the Quasi-Deuteron Model (QDM) [10] can be used to calculate the photoabsorption cross sections. The models can be used to calculate photonuclear

reaction cross sections for incident photon energies below 140 MeV which is the threshold for pion production.

The photoabsorption cross section are calculated by the GUNF [11] and GNASH codes. The GDR parameters are adjusted automatically with the GUNF code by fitting the experimental data of photoabsorption cross sections or photoneutron cross sections.

If experimental data exist for total photoabsorption cross section, it can be used to adjust the GDR parameters. For heavy nuclei, the total photoneutron cross section can be used to approximate the photoabsorption cross sections, since contributions from charged particle emission are small. But for light nuclei, this approach can not be used since charged particle emission cross sections are no longer small, and in some cases exceed the photoneutron cross section. In such cases, (γ, n) and $(\gamma, n+np)$ reaction cross sections can be used to adjust the GDR parameters with GUNF code, and at the same time charge particle emission cross sections and other photoneutron cross section can be calculated automatically with GUNF code. Then the photoabsorption cross sections can be obtained theoretically.

When the photoabsorption cross sections were established, the decay processes including neutron, proton, deuteron, triton and alpha particle emission were calculated up to 140 MeV. The spherical optical model was used to calculate the transmission coefficients. The Hauser-Feshbach theory with full angular momentum and parity conservation was used to calculate the equilibrium emission. The preequilibrium theory was used to describe the processes of preequilibrium emission, and damping to equilibrium, during the evolution of the reaction. The theory for calculating photonuclear angular distributions, enabling a determination of the double differential cross sections of ejectiles and the multiple-preequilibrium emission processes which become important when the photon energy exceeds about 50 MeV were included in the calculation.

The file of discrete level information and ground-state masses, spin and parities was provided, the mass values were based upon an interim set from Wapstra obtained prior to the 1988 publication, and supplemented in the case of unmeasured masses with values from the Moller and Nix calculations. The optical potential parameters were taken from Ref.[12] The level density parameter and the pair correction values of the first process were adjusted for some nuclei.

V. Analyses of Calculated Results for Some Isotopes

All photonuclear reaction cross sections are evaluated for the 142 isotopes of 39 elements. However, in this paper, only some selected isotopes are analysed and compared with experimental data.

^{12}C

The comparison of calculated results with experimental data [13–25] for $\gamma + ^{12}\text{C}$ reaction cross sections are given in Fig.1. The calculated photoabsorption cross sections are in good agreement with experimental data taken from Ref.[14]. The calculated results for $^{12}\text{C}(\gamma, n+np)$ reaction cross sections agree with experimental data for energy $E_\gamma < 37$ MeV, while for energy $E_\gamma > 37$ MeV, the experimental data taken from Ref.[19] are higher than the calculated results. Only three sets of experimental data for $^{12}\text{C}(\gamma, n+np)$ reaction cross sections are only given in Fig. 1. The calculated results of $^{12}\text{C}(\gamma, p)^{11}\text{B}$ reaction cross section are smaller than experimental data, but the shape of calculated cross section is the same as that of the experimental data. If the experimental data of $^{12}\text{C}(\gamma, n+np) + ^{12}\text{C}(\gamma, p)$ reaction cross sections are compared with the experimental data of photoabsorption cross section, we can see that the former results are larger than the latter for energies $E_\gamma < 50$ MeV. Therefore, the experimental data of $^{12}\text{C}(\gamma, p)^{11}\text{B}$ reaction cross sections should be checked. The calculated results of $^{12}\text{C}(\gamma, np)^{10}\text{B}$,

$^{12}\text{C}(\gamma, n\alpha)^7\text{Be}$ and $^{12}\text{C}(\gamma, p\alpha)^7\text{Li}$ reaction cross sections are larger than experimental data for low energy, respectively. However, the shapes of calculated cross section are the same as the experimental data. The cross section of $^{12}\text{C}(\gamma, 2\alpha)\alpha$ reaction is from the contribution of the fourth discrete level of ^{12}C . The calculated results of $^{12}\text{C}(\gamma, p\alpha)^7\text{Li}$ reaction cross section is also given in Fig. 1. The theoretical values of $^{12}\text{C}(\gamma, np\alpha)^6\text{Li}$ reaction cross sections are in good agreement with experimental data.

The neutron, proton, deuteron, triton, alpha particles emission and production cross sections were calculated up to 140 MeV. As seen in the fig. 1, the photoproton and photoalpha cross sections are no longer small, and for low energies the photoproton cross section exceeds the photoneutron cross sections.

^{63}Cu

The comparison of the calculated results with the experimental data [26–36] for $\gamma + ^{63}\text{Cu}$ reaction cross sections are given in Fig. 2. As seen in Fig. 2, the overall shape and the magnitude of (γ, n) , $(\gamma, 2n)$, (γ, np) and $(\gamma, n+np)$ reactions cross sections calculated are in good agreement with experimental data. The calculated results of $^{63}\text{Cu}(\gamma, p)^{62}\text{Ni}$ reaction cross sections show agreement with the experimental data for energies below 18MeV, while for energies above 18 MeV, the calculated results are smaller than the experimental data. If the calculated results of $^{63}\text{Cu}(\gamma, np+pn)^{61}\text{Ni}$ reaction cross sections are included, the calculated results would be in agreement with the experimental data. The experimental data may be the cross sections of $^{63}\text{Cu}(\gamma, xp)$ reaction. The photoneutron and total neutron production cross sections are compared with the experimental data. Since the experimental data taken from Ref.[36] are used to guide theoretical calculation, the overall shape of calculated results is in good agreement with experimental data taken from Ref.[26], while the magnitude is larger than that of experimental data. The experimental data taken from Ref.[31] are probably for (γ, n) reaction cross sections.

^{70}Ge

The comparison of calculated results with the experimental data [37–40] for the $\gamma + ^{70}\text{Ge}$ reaction cross sections are given in Fig. 3. As seen in this figure, calculated results for photoneutron cross sections are in good agreement with the experimental data taken from Refs.[38, 39]. According to the theoretical results and analysis, the experimental data taken from Ref.[39] may be (γ, xn) reaction cross sections. The theoretical results of photoabsorption cross section are basically in agreement with the experimental data taken from Ref.[37], and the calculated results of photoneutron and photoproton cross sections are compared with the experimental data taken from Refs.[37, 40].

^{154}Sm

The comparison of calculated results with experimental data [41–43] for $\gamma + ^{154}\text{Sm}$ reaction cross sections are given in Fig. 4. The overall shape and magnitude of $(\gamma, n+np)$, $(\gamma, 2n+2np)$, $(\gamma, n+np+2n+2np)$ and $(\gamma, n+np+2(2n+2np))$ reactions cross section are in good agreement with the experimental data. The theoretical results of photoabsorption cross sections for $\gamma + ^{154}\text{Sm}$ reaction are in good agreement with experimental data.

The neutron, proton, deuteron, triton, alpha particles emission and production cross sections were calculated up to 140 MeV. The calculated results show that since the photoproton and photoalpha cross sections are small, it is reasonable that the photoneutron total cross sections can be used to approximate the photoabsorption cross sections for $\gamma + ^{154}\text{Sm}$ reaction.

VI. Summary

KAERI is building a photonuclear data library, which currently includes 142 isotopes of 39 elements stored in the ENDF/B-VI format. Based on the available experimental data of photoabsorption or photoneutron cross sections, the cross sections of neutron, proton, deuteron, triton, alpha particles emission and production up to 140 MeV were evaluated. The giant dipole resonance (GDR) and the quasideuteron model (QDM) were used to calculate and evaluate the photoabsorption cross sections. The Hauser-Feshbach theory with full angular momentum and parity conservation, the preequilibrium and multiple-preequilibrium theories were used to calculate the particle emission and production cross section as well as the double differential cross sections of ejectiles. The theoretical results are basically in good agreement with the existing experimental data. Therefore KAERI photonuclear data library are reliable and are recommended for incident photon energy $E_\gamma \leq 140\text{MeV}$.

Acknowledgements

This work was performed under the auspices of Korea Ministry of Science and Technology as one of the long-term nuclear R&D programs. One of authors (Yinlu Han) acknowledges the Korea Science and Engineering Foundation for giving him an opportunity to carry out this work under the Brain Pool program, and also wishes to thank Korea Atomic Energy Research Institute for its generous hospitality.

References

- [1] Y. O. Lee, T. Fukahori, and J. Chang: Evaluation of Photoneutron Cross Sections for Ta-181 in Giant Resonance Region, in *Korean Physics Society Fall Conference, Oct. 17-18, Kwang-Un Univ., 1997*.
- [2] Y. O. Lee, T. Fukahori, and J. Chang: Evaluation of Photonuclear Reaction Data on Tantalum-181 up to 140 MeV," *J. of Nucl. Sci. and Tech.*, vol. 350, p. 685, 1998.
- [3] Y. O. Lee, Y. Han, J. Y. Lee, and J. Chang: Evaluation of Photonuclear Data of Mo, Zn, S and Cl for Medical Application, The Korean Nuclear Society Spring Meeting, May 28-29, 1999.
- [4] Y. Han: Evaluation of Photonuclear Reaction Data up to 140 MeV, *KAERI internal report* NDL-4,5,7,12,17,27,28,29, 1998-1999.
- [5] J. Y. Lee, Y. O. Lee, and J. Chang: Gamma Resonance Absorption in ^{14}N , The Korean Physical Society Spring Meeting, April 24-25, 1999.
- [6] J. Y. Lee, Y. O. Lee, and J. Chang: Analysis of Gamma Resonance Absorption in ^{14}N by Using the Radiative Direct Capture Reaction Theory, The Korean Nuclear Society Spring Meeting, May 28-29, 1999.
- [7] J. Y. Lee, Y. O. Lee, and J. Chang: Calculations of $^{13}\text{C}(p, \gamma)^{14}\text{N}$ and $^{14}\text{N}(\gamma, p)^{13}\text{C}$ Cross Sections, submitted to the Journals of Korean Physical Society.
- [8] J. Y. Lee, Y. O. Lee, J. Chang and B. T. Kim: Cross Sections for the Reaction $^{16}\text{O}(\gamma, p_3)^{15}\text{N}^*$ up to 120 MeV in the Continuum Random Phase Approximation, submitted to the Journals of Korean Physical Society.
- [9] Chadwick, M. B. et al.: Photonuclear reactions in the GNASH code. Technical Report UCRL-ID-118721, Lawrence Livermore National Laboratory, Livermore, CA (1994).

- [10] Chadwick, M. B. et al.: Pauli-Blocking in the Quasiduteron Model of Photoabsorption. *Phys. Rev., C*, **44**, 814 (1991).
- [11] Zhang, J. S.: Illustration of Photonuclear Data Cal. with GUNF Code. *Comm. of Nucl. Data Prog.*, **19**, 33 (1998).
- [12] Perey, C. M. et al.: Compilation of Phenomenological Optical Model Parameters. *Atom. Data and Nucl. Data Tables*, **17**, 1 (1976).
- [13] Burgov, N. A. et al.: Cross Section for Absorption of G-Quanta by Carbon Nuclei in the Giant Resonance Region. *Zhurnal Eksperimental'noi i Teoreticheskoi Fiziki*, **45**, 1694 (1963)
- [14] Ahrens, J. et al.: Total Nuclear Photon Absorption Cross Sections for Some Light Elements. *Nucl. Phys., A*, **251**, 479 (1975).
- [15] Fultz, S. C. et al.: Photoneutron Cross Sections for ^{12}C and ^{27}Al . *Phys. Rev.*, **143**, 790 (1966).
- [16] Lochstet, W. A. et al.: $^{12}\text{C}(\gamma, n)^{11}\text{C}$ Giant Resonance with Gamma Rays. *Phys. Rev.*, **141**, 1002 (1966).
- [17] Kneissl, U. et al.: The Quasimonoenergetic Photon Facility at the Giessen 65 MeV Electron Linear Accelerator. *Nucl. Instr. Meth. in Phys. Res., A*, **127**, 1 (1975).
- [18] Ishkhanov, B. S. et al.: Structure of the Cross Section of the Reaction $^{12}\text{C}(\gamma, n)$ in Region of the Giant Dipole Resonance. *Yadernaya Fizika*, **14**, 253 (1971).
- [19] Bazhanov, E. B. et al.: Photodisintegration of C^{12} . *Yadernaya Fizika*, **3**, 711 (1966).
- [20] Kirichenko, V. V. et al.: Reaction $^{12}\text{C}(\gamma, p)^{11}\text{B}$ at $E_{\gamma-\text{max}}=120$ MeV. *Yadernaya Fizika*, **27**, 588 (1978).
- [21] Kirichenko, V. V. et al.: Reaction $^{12}\text{C}(\gamma, p)^{11}\text{B}$ in the 40-120 MeV Energy Range. *Ukrainskii Fizichnii Zhurnal*, **22**, 959 (1977).
- [22] Khodyachikh, A. F. et al.: Correlated np Pairs from p-shell of the Carbon Nucleus. *Yadernaya Fizika*, **32**, 881 (1980).
- [23] Kirichenko, V. V. et al.: Study of Reactions $^{12}\text{C}(\gamma, p+\alpha)^7\text{Li}$ at $E_{\gamma-\text{max}}=120$ MeV. *Yadernaya Fizika*, **29**, 572 (1979).
- [24] Murakami, A. et al.: $^6\text{Li}(\gamma, t)\text{He}^3$ and $^6\text{Li}(\gamma, p+d)\text{H}^3$ Reactions. *Japan Phys. J.*, **28**, 1 (1970).
- [25] Dogyust, I. V. et al.: Correlation Effects in the $^{12}\text{C}(\gamma, p+n+\alpha)^6\text{Li}$ Reaction in the Range of Intermediate Energies. *Ukrainskii Fizichnii Zhurnal*, **10**, 1465 (1982).
- [26] Fultz, S. C. et al.: Photoneutron Cross Sections for Natural Cu, Cu^{63} and Cu^{65} . *Phys. Rev., B*, **133**, 1149 (1964).
- [27] Scott, M. B. et al.: Electro- and Photodisintegration Cross Sections of Cu^{63} . *Phys. Rev.*, **100**, 209 (1955).
- [28] Sund, R. E. et al.: Measurements of the $^{63}\text{Cu}(\gamma, n)$ and $(\gamma, 2n)$ Cross Sections. *Phys. Rev.*, **176**, 1366 (1968).

- [29] Berman, A. I. et al.: Absolute Cross Section Versus Energy of the $^{63}\text{Cu}(\gamma, n)$ and $^{63}\text{Cu}(\gamma, 2n)$ Reactions. *Phys. Rev.*, **96**, 83 (1954).
- [30] Dzhilavyan, L. Z. et al.: Study of the Cross Section of the Reaction $^{63}\text{Cu}(\gamma, n)$ in the Beam of Quasimonochromatic Annihilation Photons in Energy Range from 12 to 25 MeV. *Yadernaya Fizika*, **30**, 294 (1979).
- [31] Katz, L. et al.: The Solution of X-ray Activaton Curves for Photonuclear Cross Sections. *Canada J. Phys.*, **29**, 518 (1951).
- [32] Jeong, S. C. et al.: Cross Section Measurement for the $^{63}\text{Cu}(\gamma, n)^{62}\text{Cu}$ Reaction. *J. Korea Phys. Soc.*, **17**, 539 (1984).
- [33] Bianco, W. E. DEL et al.; Photonuclear Activation by 20.5 MeV Gamma Rays. *Phys. Rev.*, **126**, 709 (1962).
- [34] Nakamura, T. et al.: Absolute Cross Sections of the (γ, n) Reaction for Cu^{63} , Zn^{64} and Ag^{109} . *Japan Phys. J.*, **14**, 693 (1959).
- [35] Coote, G. E. et al.: Cross Sections for the (γ, n) Reaction in ^{63}Cu , ^{65}Cu , ^{64}Zn , ^{121}Sb and ^{141}Pr , Measured with Monochromatic Gamma Rays. *Nucl. Phys.*, **23**, 468 (1961).
- [36] Varlamov, V. V. et al.: The $\text{Cu}^{63,65,\text{nat}}(\gamma, np)$ Reaction Cross Sections in the Giant Dipole Resonance Region. *Voprosy Atomnoi Nauki i Tekhniki, Seriya: Yadernye Konstanty*, **2**, 1 (1995).
- [37] Mccarthy, J. J. et al.: Systematic Study of the Photodisintegration of Ge^{70} , Ge^{72} , Ge^{74} , and Ge^{76} . *Phys. Rev., C*, **11**, 772 (1975).
- [38] Carlos, P. et al.: A Study of the Photoneutron Contribution to the Giant Dipole Resonance of Nuclei in the $64 \leq A \leq 86$ Mass Region. *Nucl. Phys., A*, **258**, 365 (1976).
- [39] Goryachev, A. M. et al.: The Studing of the Photoneutron Reactions Cross Sections in the Region of the Giant Dipole Resonance in Zinc, Germanium, Selenium, and Strontin Isotopes. *Voprosy Teoreticheskoy Yadernoj Fiziki*, **8**, 121 (1982).
- [40] Mccarthy, J. J. et al.: Isospin Components of the Giant Dipole Resonance in Several Germanium Isotopes. *Nucl. Phys., A*, **213**, 371 (1973).
- [41] Carlos, P. et al.: The Giant Dipole Resonance in the Transition Region of the Samariam Isotopes. *Nucl. Phys., A*, **225**, 171 (1974).
- [42] Gurevich, G. M. et al.: On the Width of E1-Giant Dipole Resonance for Deformed Nuclei in $A=150-186$ Region. *Zhurnal Eksperimental'noi Teoreticheskoi Fiziki, Pisma v Redakciyu*, **28**, 168 (1978).
- [43] Gurevich, G. M. et al.: Total Nuclear Photoabsorption Cross Sections in the Region $150 < A < 190$. *Nucl. Phys., A*, **351**, 257 (1981).

Table 1. Adopted ENDF/B-VI format for photonuclear data

MF	MT	Explanation
1	451	Descriptive information and dictionary
3	3	Total photoabsorption cross section
	4	Total (γ , 1n) cross section
	5	Photoabsorption cross section from which production c.s. for particles and isotopes are determined using yields in MF6/MT5
	12	Total (γ , 2nt+3nd+4np) cross section
	16	Total (γ , 2n) cross section
	17	Total (γ , 3n) cross section
	22	Total (γ , n α +3n2p) cross section
	24	Total (γ , 2n α +4n2p) cross section
	25	Total (γ , 3n α +5n2p) cross section
	28	Total (γ , np+d) cross section
	32	Total (γ , 2np+nd+t) cross section
	33	Total (γ , 3np+2nd+nt) cross section
	37	Total (γ , 4n) cross section
	43	Total (γ , 5n) cross section
	44	Total (γ , n2p) cross section
	103	Total (γ , p) cross section
	107	Total (γ , α +2n2p) cross section
	111	Total (γ , 2p) cross section
	201	Total (γ , 6n) cross section

	209	Total (γ , 14n) cross section
	212	Total (γ , 5np+4nd+3nt) cross section
	215	Total (γ , 6np+5nd+4nt) cross section
	218	Total (γ , 7np+6nd+5nt) cross section
	221	Total (γ , 8np+7nd+6nt) cross section
	224	Total (γ , 9np+8nd+7nt) cross section
	227	Total (γ , 10np+9nd+8nt) cross section
	230	Total (γ , 11np+10nd+9nt) cross section
	233	Total (γ , 12np+11nd+10nt) cross section
	236	Total (γ , 13np+12nd+11nt) cross section
	243	Total (γ , 4n α +6n2p) cross section
	245	Total (γ , 5n α +7n2p) cross section
	247	Total (γ , 6n α +8n2p) cross section
	249	Total (γ , 7n α +9n2p) cross section
	251	Total (γ , 8n α +10n2p) cross section
	253	Total (γ , 9n α +11n2p) cross section
	255	Total (γ , 10n α +12n2p) cross section
6	5	Production cross section and energy-angle distributions for emission neutrons, protons, deuterons, and alphas; and angle-integrated spectra for gamma rays and residual nuclei that are stable against particle emission

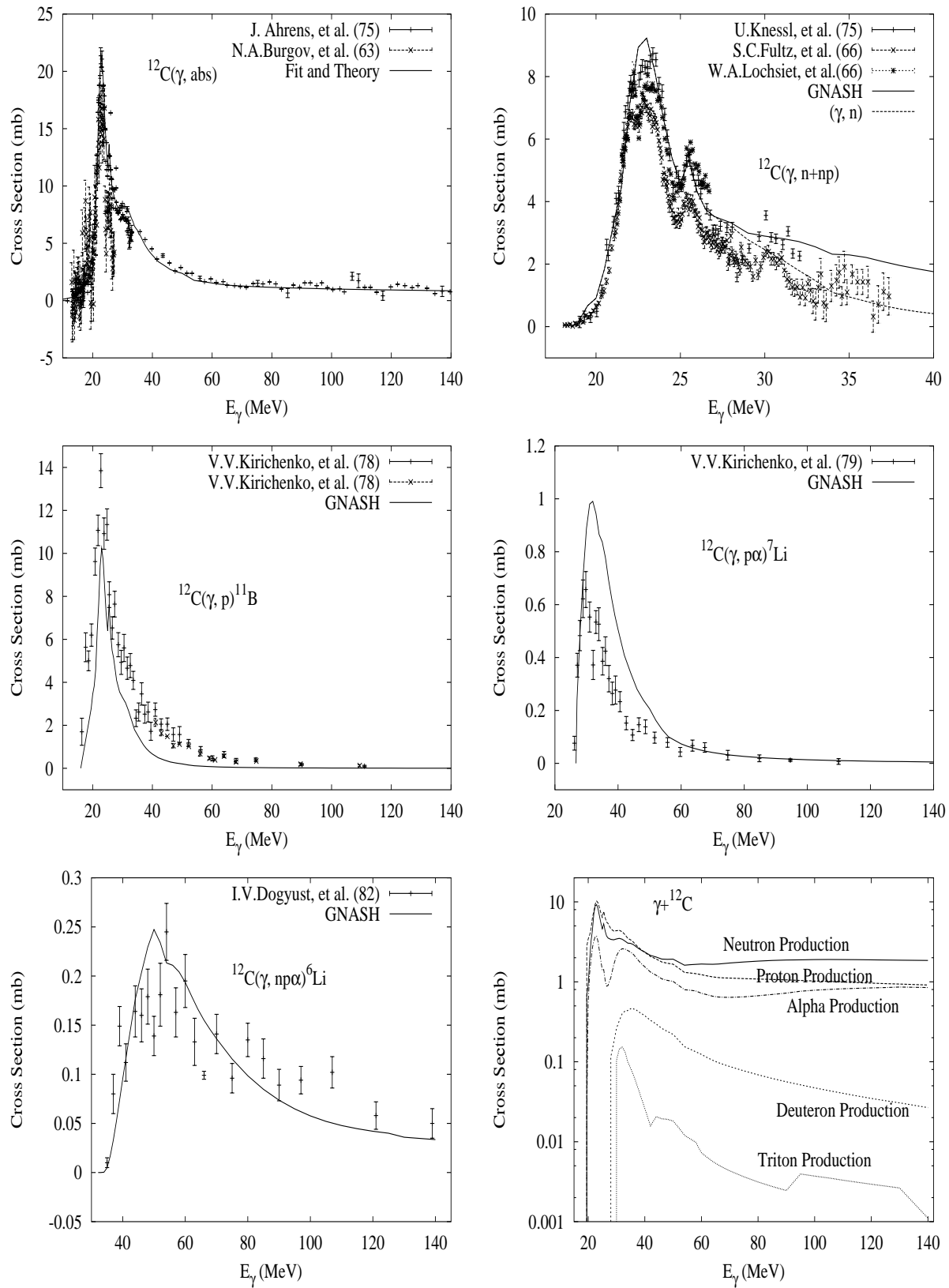


Figure 1: The comparison of calculated results with experimental data for ^{12}C photonuclear reaction cross sections

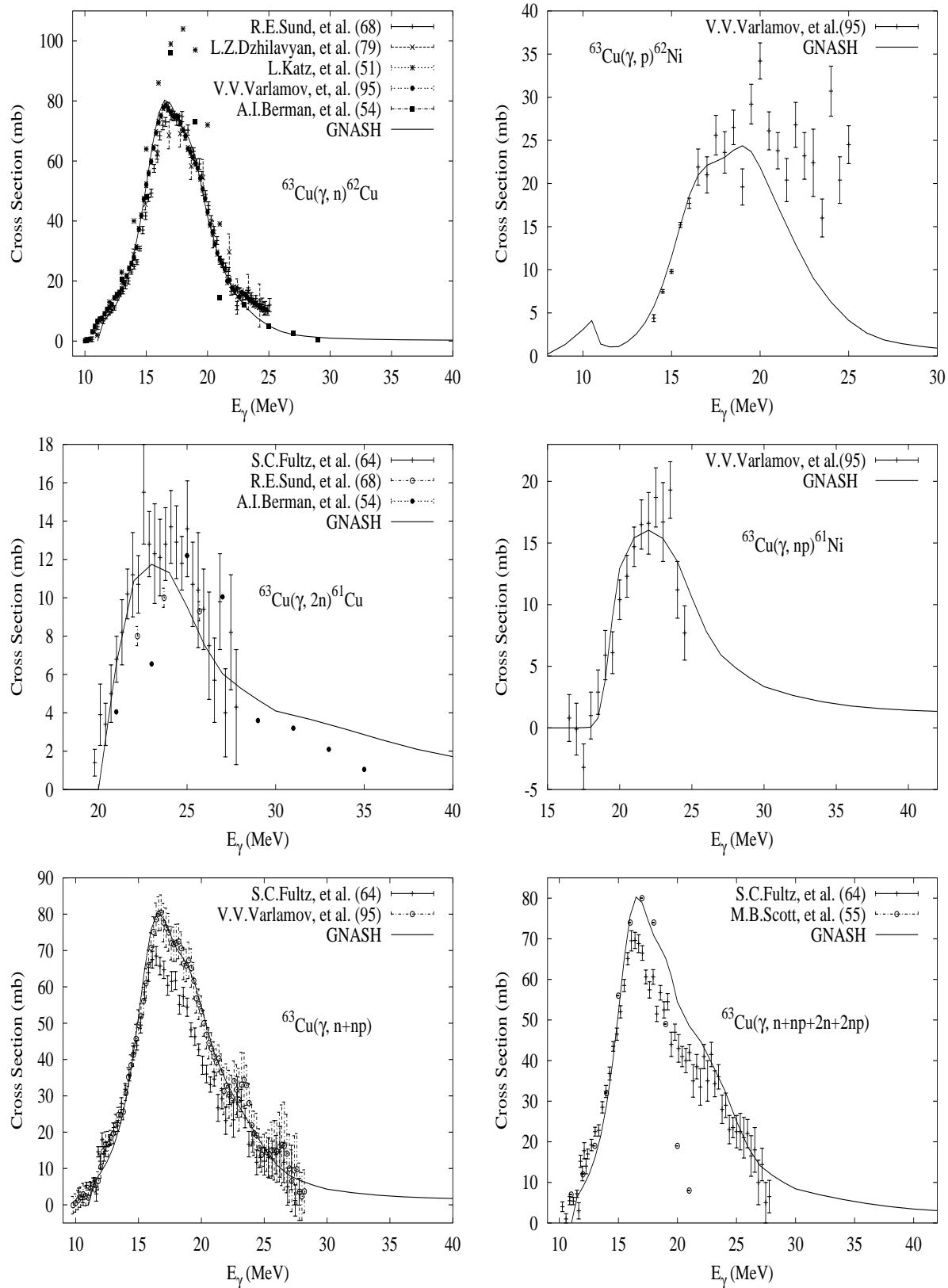


Figure 2: The comparison of calculated results with experimental data for ^{63}Cu photonuclear reaction cross sections

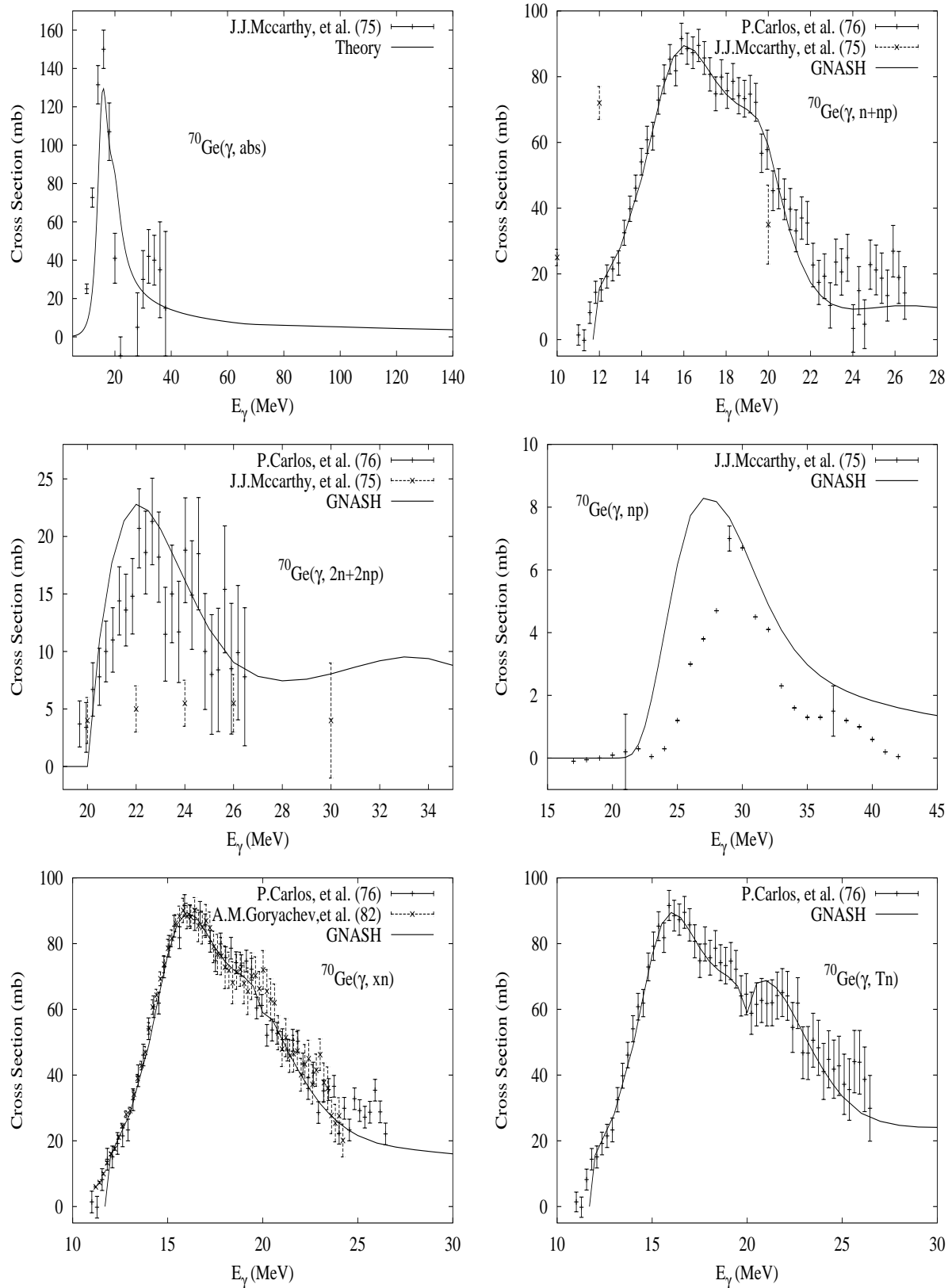


Figure 3: The comparison of calculated results with experimental data for ^{70}Ge photonuclear reaction cross sections

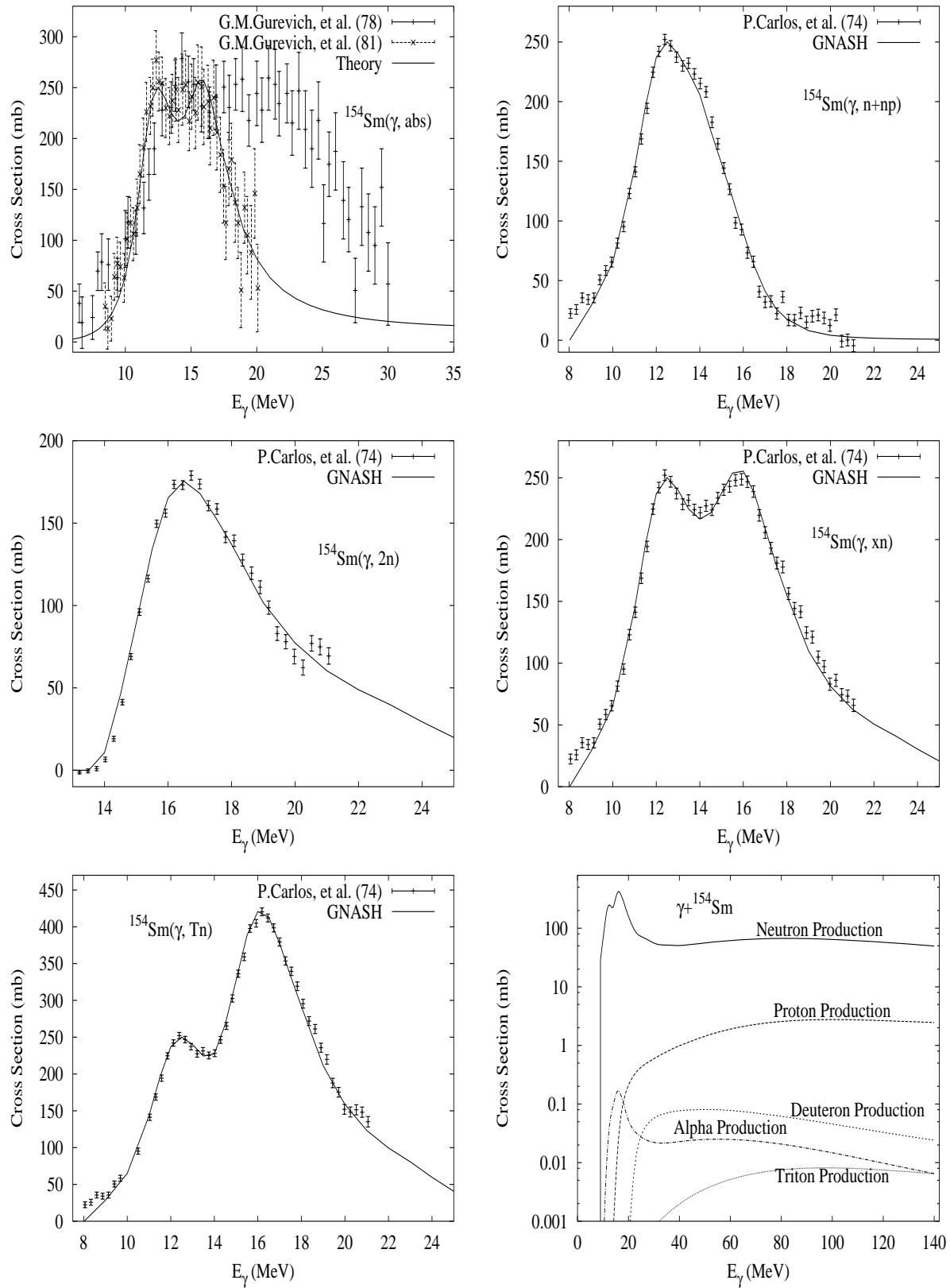


Figure 4: The comparison of calculated results with experimental data for ^{154}Sm photonuclear reaction cross sections